in a drybox. The viscometer constant, $\mathbf{C} = (hrg\rho)/2lV$, was determined by using viscosity standards provided by the Cannon Instrument Co. (*9*). To assure acceptable accuracy, the bath temperature was controlled to within ±0.01 °C and the time to within ±0.1 s.

Results. Kinematic viscosities of $SOCl_2$-based electrolytes were determined as a function of LiCl concentration (X_{LiCl}, M) and temperature (T, °C). Results are summarized in Tables VIII–XIII.

Densities

The density of any substance is the measure of the weight to volume ratio. A number of methods were devised to measure the density of liquids (*8*). Among them are pycnometric methods, dilatometers, hydrostatic balance, magnetic float, and buoyancy technique.

Experimental Procedure. The densities of the $SOCl_2$-based electrolytes were determined in Pyrex dilatometers whose volumes have been calibrated with methanol and distilled water. The accuracy within ±0.0001 g cm^{-3} is routinely obtained.

Results. Densities of $SOCl_2$-based electrolytes were determined as a function of LiCl concentration and temperature. Results are summarized in Tables XIV–XVIII.

Acknowledgment

We thank Mr. Maurice Murphy (NAVSEA 63R-32) and Dr. R. Lazar, Naval Underwater Systems Center, Rhode Island, Code 36301, for their interest and support.

Literature Cited

(1) Auburn, J. J.; French, K. W.; Lieberman, S. I.; Shah, V. K.; Heller, A. *J. Electrochem. Soc.* **1973**, *120*, 1613.
(2) Dey, A. N.; "Primary Li/$SOCl_2$ Cells XI: Performance and Safety of Super High Rate Li/$SOCl_2$ Batteries", 12th International Power Source Symposium, Brighton, 1980.
(3) Driscoll, J. R.; Szpak, S. *Proc.—Power Sources Symp.* **1982**, in press.
(4) Jones, G.; Bradshah, B. C. *J. Am. Chem. Soc.* **1933**, *55*, 1780.
(5) Washburn, E. W. *J. Am. Chem. Soc.* **1916**, *38*, 2431.
(6) Robinson, R. A.; Stokes, R. H. "Electrolyte Solutions", 2nd ed.; Academic Press: New York, 1959.
(7) Venkatasetty, H. V. *J. Electrochem. Soc.* **1975**, *122*, 245.
(8) Johnson, J. F.; Martin, J. R.; Porter, R. S. In "Techniques of Chemistry"; Weissberger, A., Rossiter, B. W., Eds.; Wiley: New York, 1977; Vol. I, Part VI.
(9) Cannon Instrument Co., State College, PA, Bulletin, No. 90.

Received for review February 22, 1982. Revised manuscript received July 21, 1982. Accepted August 9, 1982. This work was funded by Naval Sea Systems Command (NAVSEA 63R-32) through a propulsion block program and constitutes a fraction of a major program to establish a technology base for high rate discharge Li/$SOCl_2$ batteries.

Vapor–Liquid Equilibria for the Carbon Dioxide–1-Butene System at 37.7 and 45.0 °C

Paul K. Behrens† **and Stanley I. Sandler***
Department of Chemical Engineering, University of Delaware, Newark, Delaware 19711

A new high-pressure vapor–liquid equilibrium cell is described. Data taken with this cell for the CO_2–*n*-butane system at 37.7 °C are found to be in good agreement with those previously reported for this mixture. Data are also reported for the CO_2–1-butene system at 37.7 and 45.0 °C. All three sets of data were found to be correlated equally well by the Peng–Robinson, Soave–Redlich–Kwong, and Teja–Patel equations of state. Binary interaction parameters obtained by correlating our data are reported for each of these equations, and estimates of the critical points of CO_2–*n*-butane and CO_2–1-butene mixtures are given.

Introduction

Present interest in tertiary oil recovery by carbon dioxide flooding and synthetic fuels processing has encouraged us to initiate an experimental research program on the vapor–liquid equilibrium of carbon dioxide–hydrocarbon systems. Here we report the first results of this program which include the construction of a high-pressure vapor–liquid cell, the testing of our equipment by measuring vapor–liquid equilibrium data for a system (CO_2–*n*-butane) for which data have been published by others (*1*), and data for the CO_2–1-butene mixture over a range of conditions which have not been previously available (*2*). We also report on the fitting of our data with three different equations of state, and the estimation of mixture critical points for the systems studied.

Equipment

The heart of our equipment is a stirred, vapor and liquid recirculation equilibrium cell, shown in Figure 1. The cell is a large (1 L) autoclave manufactured by Autoclave Engineers, Inc., with a Magnedrive magnetically coupled stirrer driven by an external motor. To ensure the rapid attainment of vapor–liquid equilibrium, both the vapor and liquid phases are recirculated by using magnetically driven double-acting pumps constructed by us.

These pumps, shown in detail in Figure 2, consist of a barrel and heads constructed of nonmagnetic 316 stainless steel and a piston of magnetic 410 stainless steel. The piston, shown in Figure 3, has two Teflon rings and is driven by two electromagnet coils wrapped on the barrel of the pump. The magnetic field generated by the coil passes through the 316 stainless-steel barrel, to force the piston up or down depending on the coil being energized. A solid-state timer/power supply which we built pulses the coils in partially overlapping cycles so that the piston is decelerated near the end of its stroke. This provides pumping action while minimizing the piston–pump head contact at the end of each stroke. As indicated in Figures 2 and 3, four gravity-operated check values ensure the unidirectional flow of the pumped fluid with this dual-acting pump. Circulation of the phases using these pumps is confirmed in two ways. First, when the cell head is removed, the circulation of both phases is visually observed (indeed, this procedure is used to determine the optimum piston ring clearance). Second,

---

[†] Present address: Amoco Chemicals Corp., Amoco Research Center, Naperville, IL 60566.

0021-9568/83/1728-0052$01.50/0

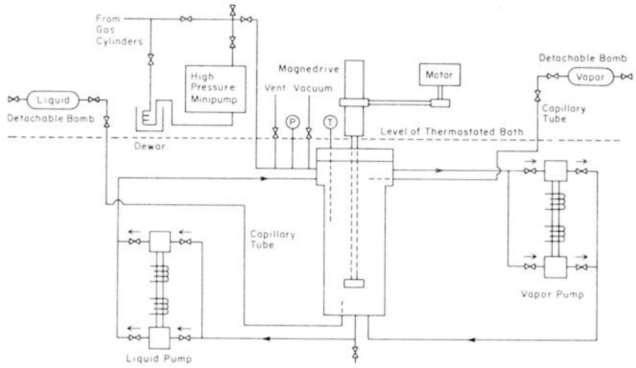

Figure 1. Schematic diagram of the vapor–liquid equilibrium equipment used in this work.

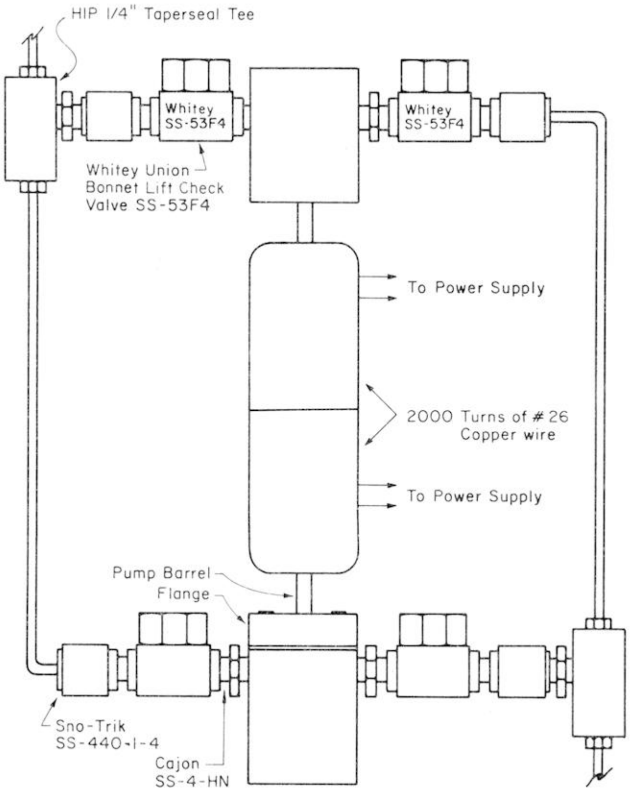

Figure 2. Detailed diagram of the electromagnetic pump constructed by us and used in this work.

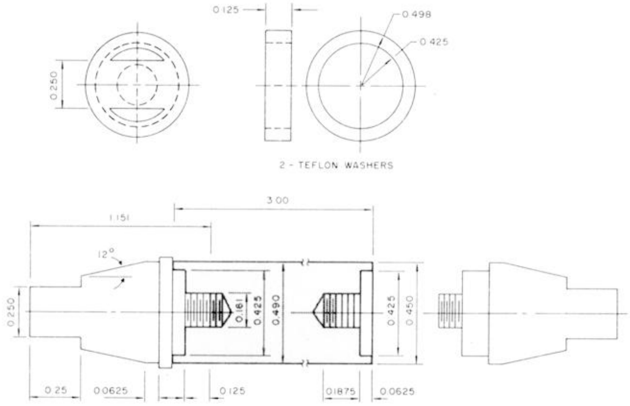

Figure 3. Detailed diagram of the piston assembly used in the electromagnetic pumps.

during operation, an electronic stethoscope is used to detect the piston movement, and hence pumping. To maintain temperature, one immerses the entire system (cell and pumps) in a large (75 gal) oil bath filled with Mobiltherm 603 heat transfer fluid. The temperature of the oil bath, and therefore the system, is controlled by a specially designed proportional controller constructed in the instrument shop of the College of Engineering at the University of Delaware, and electric heating elements. A 0.75-hp agitator with two 6-in. propellers was used to thoroughly agitate the oil bath. The use of vigorous mixing in such a large oil bath served to dampen changes in temperature and thus allowed the temperature to be controlled at ±0.02 °C. The temperature range obtainable with the present setup is 10–100 °C. (The subambient temperature is obtained by circulating cold water through the large coil of copper tubing located in the rear section of the oil bath.)

The cell temperature was monitored by using a platinum resistance element located in the thermowell of the equilibrium cell. The probe is read with a Hewlett-Packard 2802A digital temperature readout. Good thermal contact between the well and the element was achieved by filling the well with Dow Corning 200 silicone oil. The precision in readings of this temperature system was 0.01 °C. The system was calibrated with an ASTM mercury thermometer.

The cell pressure was monitored with a BLH Model DH strain gauge type pressure transducer. This was read with a BLH Model 450A digital readout. The strain gauge pressure transducer/readout was calibrated with an Amtek Mansfield and Green Division, 0–5000-psi dead-weight tester (Model DM-T-50). This allowed the pressure to be known to ±0.3%.

Though several types of sampling were tried (in-line sampling bombs and gas-chromatographic sampling valves), we have found the sampling using fine capillary tubes in the vapor and liquid phases, separate from the recirculation loops, to be the most satisfactory. To obtain samples, we turned off the vapor and liquid recirculation pumps and agitator after a sufficiently long time (4–8 h) that equilibrium was achieved (as evidenced by constant cell pressure), and, after a short period, the sample lines were purged, and samples taken in evacuated sample bombs. Due to the large size of our cell, the small volume removed for purging and sampling (about 2×10^{-3} L at cell conditions), and the time scale for reequilibration in a stagnant system, we are confident that equilibrium samples were obtained. All sample lines and the sample bombs were heated to avoid problems of partial condensation or compositional inhomogeneities.

Composition measurements were made with an Antek Model 300 gas chromatograph with thermal conductivity detector and a Spectra-Physics Minigrator. The gas-chromatographic columns used were 6 ft × 0.125 in. stainless steel packed with 200 mesh Porpak Q. Helium carrier gas flowed through both the sample and reference columns at a rate of 25 cm^3/min, and the columns were maintained at a temperature of 135 °C. The sample bombs were heated for 4 h or more after a sample was obtained to ensure that there was a homogeneous composition in the bomb. A thermostated sample handling box was added to the gas chromatograph which allowed direct connection of the sample bomb, evacuation of the connecting lines, and then the addition of a sample of precisely regulated pressure (0.6 kPa, independent of system pressure), fixed volume (as determined by the volume of the sampling value), and temperature.

The operation of the gas chromatograph was calibrated by using the response factor method with known amounts of pure components. With the sample handling box, the sample pressure could be varied during the calibration to determine the range over which the detector response was linear with sample size. The calibration of the gas chromatograph–detector unit was then checked in two ways: first, with a commercially (Matheson) prepared mixture of the components that we were using which had a reported compositional accuracy of ±0.02% absolute, and with mixtures prepared in our laboratory by using

Table I. Original Experimental Data for the CO_2/*n*-Butane System at 37.7 °C

temp, K	press., MPa	x_{CO_2}	y_{CO_2}
310.85	0.9580	0.0684	0.5488
310.85	1.0568	0.0739	0.5824
310.84	1.5966	0.1438	0.7092
310.85	2.3537	0.2230	0.7877
310.84	2.6765	0.2900	0.7884
310.85	2.8245	0.3200	0.8342
310.82	2.8740	0.3025	0.8236
310.83	3.4236	0.4020	0.8780
310.84	3.9615	0.4342	0.8746
310.81	4.9437	0.5826	0.8867
310.84	5.5791	0.6864	0.8946
310.84	5.9724	0.7536	0.9195
310.86	6.1923	0.7855	0.9157
310.84	7.1303	0.8708	0.9408

Table II. Original Experimental Data for the CO_2/1-Butene System at 37.7 °C

temp, K	press., MPa	x_{CO_2}	y_{CO_2}
310.84	0.6202	0.0246	0.2188
310.87	0.8773	0.0584	0.4865
310.85	1.4291	0.1345	0.6760
310.89	1.4597	0.1456	0.6953
310.83	1.8326	0.1900	0.7451
310.84	2.0984	0.2292	*a*
310.85	2.3015	0.2575	*a*
310.87	2.3284	0.2561	0.7924
310.83	2.5576	0.2854	0.8099
310.84	2.8669	0.3504	0.8303
310.82	2.9152	0.3447	0.8468
310.87	3.3360	0.3979	0.8602
310.82	3.4990	0.4316	0.8607
310.80	4.4511	0.5659	0.8953
310.85	4.5326	0.5812	0.8921
310.85	4.9500	0.6328	0.9006
310.83	5.2778	0.6859	0.9167
310.79	5.3711	*a*	0.9227
310.88	5.5700	0.7248	0.9113
310.78	5.7611	0.7500	0.9163
310.85	6.3394	0.8182	0.9075

[a] Sample lost.

a specially constructed gas mixer. In brief, a gas mixture of known composition was prepared by sequentially adding the two gases to a thermostated and initially evacuated sample bomb. The pressure in the sample bomb was accurately measured following each gas addition by using a Heise Model 710 pressure meter (with an accuracy of ±0.1%) after a sufficiently long time had elapsed for thermal reequilibration. The maximum pressure in the sample bomb was kept below 0.3 MPa, so that the gas composition in the bomb could be computed from the measured pressures by using the ideal gas law. On the basis of these prepared mixtures, we estimate that the standard deviation in our composition measurements is approximately 0.005 mole fraction.

Finally, the fluids to be used were loaded into the initially evacuated equilibrium cell either directly from gas tanks or by using a Milton-Roy Model 396 Minipump, depending on the cell pressure. In the results reported here, instrument-grade carbon dioxide from Airco and high-purity *n*-butane from Matheson and 1-butene from Phillips were used as received.

Results and Discussion

In Tables I–III we report our original, unsmoothed data for the CO_2–*n*-butane system at 37.7 °C and for the CO_2–1-butene system at 37.7 and 45 °C, respectively. The data for the CO_2–*n*-butane system were the first taken with the new cell, and as such were taken over a period of several months as we refined our technique. This accounts for the larger scatter in this data set than in the CO_2–1-butene data sets taken later.

Table III. Original Experimental Data for the CO_2/1-Butene System at 45 °C

temp, K	press., MPa	x_{CO_2}	y_{CO_2}
318.15	0.5171	0.0000	0.0000
318.19	0.7488	0.0270	0.3321
318.18	1.2707	0.0920	*a*
318.13	1.7656	0.1472	0.6671
318.14	1.9174	0.1712	*a*
318.12	2.0268	0.1909	*a*
318.14	2.2049	0.2088	*a*
318.15	2.8178	0.2741	0.7803
318.14	3.4650	0.3661	0.8304
318.15	3.5500	0.3955	0.8358
318.15	3.8357	0.4188	0.8397
318.11	4.0713	0.4454	0.8370
318.16	4.3000	0.4754	0.8527
318.17	4.6500	0.5300	0.8973
318.15	5.0955	0.5784	0.8775
318.14	5.6920	0.6632	0.8871
318.17	5.9238	0.6916	0.9020
318.16	6.1968	0.7165	0.9243
318.13	6.5900	0.7648	0.9026
318.16	6.6660	0.7698	0.9135
318.13	6.9500	0.8150	0.9061
318.16	6.9562	0.8035	0.9228
318.14	7.3472	0.8450	0.9178

[a] Sample lost.

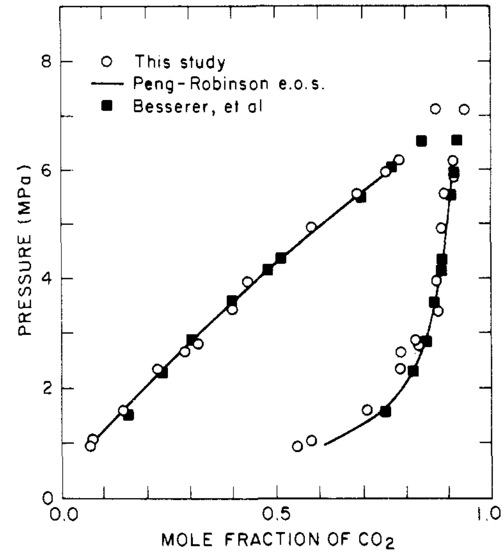

Figure 4. Experimental data and Peng–Robinson equation of state results for the carbon dioxide–*n*-butane system at 37.7 °C (k_{ij} = 0.125).

Because of the difference in density between the vapor and liquid phases, the effect of entrainment on composition is greater in the vapor than in the liquid phase. For this reason, in reported vapor–liquid equilibrium data, vapor-phase compositions are generally less accurate than those for the liquid phase. Though we believe we have eliminated entrainment, we too find more scatter in our vapor-phase compositions.

In Figure 4 we compare our results for the CO_2–*n*-butane system at 37.7 °C with those previously reported by Besserer and Robinson (*1*). Except at the lowest pressures, the agreement is very good.

We have correlated our data using three cubic equations of state: the two-constant Peng–Robinson (*3*)

$$P = \frac{RT}{v - b} - \frac{a(T)}{v(v + b) + b(v - b)} \tag{1}$$

and Soave–Redlich–Kwong (*4*)

$$P = \frac{RT}{v - b} - \frac{a(T)}{v(v + b)} \tag{2}$$

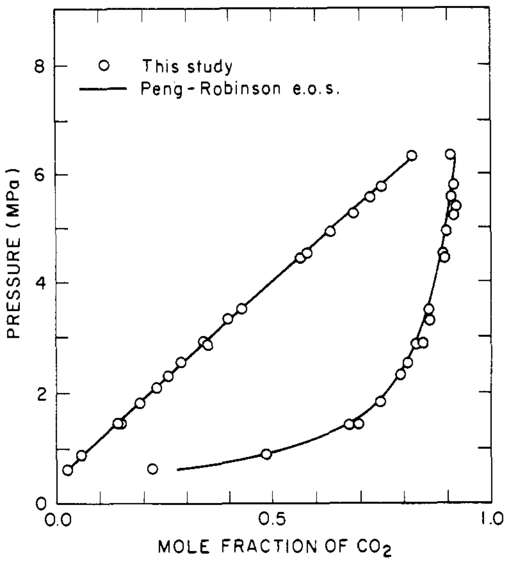

Figure 5. Experimental data and Peng-Robinson equation of state results for the carbon dioxide-1-butene system at 37.7 °C (k_{ij} = 0.086).

Table IV. Binary Interaction Parameters for the CO_2-Hydrocarbon Systems of This Study Using Different Equations of State

	k_{12}		
	CO_2-n-C_4H_{10},	CO_2-1-C_4H_8	
eq of state	T = 37.7 °C	T = 37.7 °C	T = 45.0 °C
Peng-Robinson	0.125	0.086	0.089
Soave-Redlich-Kwong	0.134	0.091	0.095
Teja-Patel	0.129	0.089	0.093

equations of state and the three-constant Teja-Patel equation (*5*)

$$P = \frac{RT}{v - b} - \frac{a(T)}{v(v + b) + c(v - b)} \qquad (3)$$

where P is the pressure, R is the gas constant, T is the temperature, and v is the molar volume.

The generalized expressions for the parameters b and c and the temperature-dependent function a for each of these equations were used and can be found in the original references (*3-5*). The van der Waals one-fluid mixing rules were used in the correlation

$$a = \sum_{ij}\sum x_i x_j a_{ij} \qquad (4)$$

$$b = \sum_i x_i b_i \qquad (5)$$

$$c = \sum x_i c_i \qquad (6)$$

with

$$a_{ij} = (a_{ii} a_{jj})^{1/2}(1 - k_{ij}) \qquad (7)$$

where k_{ij} is the binary interaction parameter obtained by fitting experimental data. We used a fitting procedure which optimized the choice of k_{ij} by minimizing the least-squares error in the bubble-point pressure using the experimental temperature and liquid-phase composition as the input data. The vapor-phase composition was not used in the fitting because of the presumed greater error in these data.

Figures 4-6 show our data, together with the best bubble-point fit of the data using the Peng-Robinson equation of state. On the scale of this graph, the results of using the three different equations of state are indistinguishable. The binary interaction parameters for each equation and data set are given in Table IV. Figure 7 presents a plot of the deviations between the predicted and measured pressures and vapor-phase mole fractions for the CO_2-1-butene system at 37.7 °C using the Peng-Robinson equation of state. (Similar plots using the other equations of state are virtually indistinguishable from the one shown.)

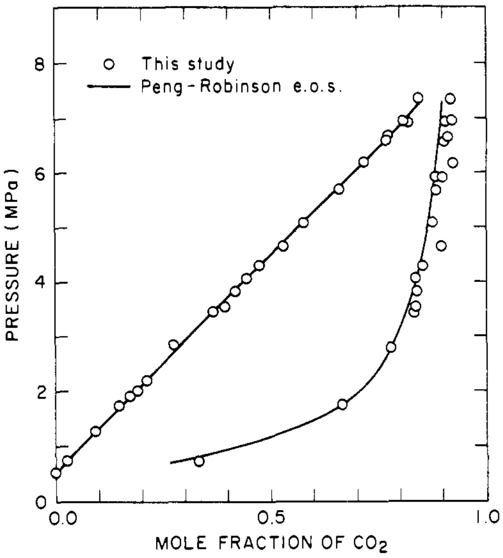

Figure 6. Experimental data and Peng-Robinson equation of state results for the carbon dioxide-1-butene system at 45.0 °C (k_{ij} = 0.089).

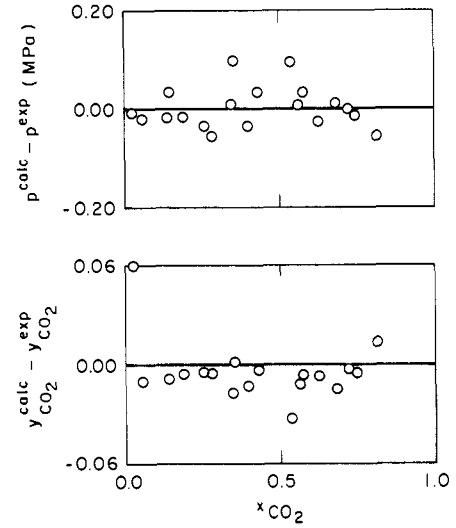

Figure 7. Deviations between the experimental data and calculated results using the Peng-Robinson equation of state for the carbon dioxide-1-butene system at 37.7 °C.

One observation from this fitting is that each of the equations of state used represents the experimental data with approximately equal accuracy, though with slightly different values for the binary interaction parameter. This may seem surprising since one expects that, for the systems studied, the Teja-Patel equation should best fit the liquid densities, and the Soave-Redlich-Kwong equation, while still satisfactory, is likely to provide the least accurate fit. This indistinguishability in vapor-liquid predictions may be explained by noting that the fugacity of a species in a mixture, $\bar{f}_i$, is related to the equation of state as follows (*6*):

$$RT \ln \frac{\bar{f}_i(T,P,x_i)}{x_i P} = \frac{1}{RT}\int_{v=\infty}^{v}\left[\frac{RT}{v} - N\left[\frac{\partial P}{\partial N_i}\right]_{T,v,N_{j\neq i}}\right] dv - \ln\frac{Pv}{RT}$$

Table V. Estimated Mixture Critical Points Using the Peng-Robinson Equation of State with the Binary Interaction Parameter Determined from Our Data

	$x^c_{CO_2}$	critical press., MPa
CO_2-*n*-butane at 37.7 °C	0.925	72.25
CO_2-1-butene at 37.7 °C	0.940	73.75
CO_2-1-butene at 45.0 °C	0.887	75.07

where N_i is the mole number of species i. Thus, while the species fugacity involves an integral over volume, a differentiation with respect to mole number (or mole fraction) is required. Therefore, the species fugacities, and thus the phase equilibrium predictions, are much more sensitive to the mixing rule and the binary interaction parameter used than they are to the equation of state in predicting specific volumes or densities. Consequently, it is not surprising that all the equations of state considered here yield similar phase equilibrium predictions.

Finally, for enhanced oil recovery or supercritical extraction processes, it would be useful to have estimates of the critical points of each of the mixtures studied. Rather than trying to establish the critical mixture compositions and pressures for the temperatures of our data sets by extrapolation, we have used the Peng-Robinson equation of state with the previously determined binary interaction parameters, and the critical point calculational method of Michelsen and Heidemann (*7*, *8*), even though cubic equations of state are not especially accurate in the critical region. The results appear in Table V.

Glossary

a, b, c	equation of state constants
$\bar{f}_i$	species fugacity
k_{ij}	binary interaction coefficient
N	number of moles
P	pressure
R	gas constant
T	temperature
v	molar volume
x	liquid-phase mole fraction
y	vapor-phase mole fraction

Registry No. CO_2, 124-38-9; 1-butene, 106-98-9; butane, 106-97-8.

Literature Cited

(1) Besserer, G. J.; Robinson, D. B. *Can. J. Chem. Eng.* **1971**, *26*, 651.
(2) Nagahama, K.; Konishi, H.; Hoshino, D.; Hirata, M. *J. Chem. Eng. Jpn.* **1974**, *7*, 323.
(3) Peng, D.-Y.; Robinson, D. B. *Ind. Eng. Chem. Fundam.* **1976**, *15*, 59.
(4) Soave, G. *Chem. Eng. Sci.* **1972**, *27*, 1197.
(5) Patel, N. C.; Teja, A. S. *Chem. Eng. Sci.* **1982**, *37*, 463.
(6) Prausnitz, J. M. "Molecular Thermodynamics of Fluid-Phase Equilibria"; Prentice-Hall: Englewood Cliffs, NJ, 1969; p 89.
(7) Heidemann, R. A.; Khalil, A. M. *AIChE J.* **1980**, *26*, 769.
(8) Michelsen, M. L.; Heidemann, R. A. *AIChE J.* **1981**, *27*, 521.

Received for review March 5, 1982. Revised manuscript received September 3, 1982. Accepted September 30, 1982. We gratefully acknowledge funds provided by Air Products and Chemicals Corp., the Chevron Oil Field Research Co., the Mobil Foundation, and the University of Delaware which allowed this equipment to be built. P.K.B. also is pleased to acknowledge the financial support that he received as a graduate student from the Department of Chemical Engineering of the University of Delaware.

Enthalpy of Dilution of Aqueous Solutions of Na_2SO_4, K_2SO_4, and $MgSO_4$ at 373.15 and 423.65 K and of $MgCl_2$ at 373.15, 423.65, and 472.95 K

James E. Mayrath[†] **and Robert H. Wood***
Department of Chemistry, University of Delaware, Newark, Delaware 19711

The enthalpies of dilution of aqueous solutions of $MgCl_2$, Na_2SO_4, and $MgSO_4$ have been measured at temperatures of 373.15 and 423.65 K. In addition, $MgCl_2$ has also been measured at 472.95 K. These measurements, together with literature data at lower temperatures, have been used to calculate reliable values of the relative apparent molar enthalpy, L_ϕ, the difference in osmotic coefficient on going from 298.15 K to T, $\phi(T) - \phi(298.15\text{ K})$, and the logarithm of the ratio of activity coefficients at T and 298.15 K, $\ln[\gamma(T)/\gamma(298.15\text{ K})]$ for both aqueous $MgCl_2$ and Na_2SO_4. The results are in reasonable agreement with other data from the literature.

Introduction

The measurements reported here are part of a continuing investigation of the thermodynamic properties of aqueous salt solutions at high temperatures using flow calorimetry (*1*, *2*). This paper represents enthalpy of dilution data for several electrolytes containing divalent ions. From these data and previous room-temperature measurements, the osmotic and activity coefficients of $MgCl_2$ and Na_2SO_4 have been calculated up to 473 and 423 K, respectively.

Experimental Section

Calorimeter. The flow calorimeter used in these experiments and its method of operation have been described in detail elsewhere (*2*, *3*). The accuracy of the calorimeter is approximately 1% and the temperatures of experiments are accurate to about 0.3 K. The pressures were kept constant at 0.1–0.3 MPa greater than the water vapor pressure at the experimental temperature.

Solutions. All solutions were prepared from Fisher certified reagent salts. The purities listed by the manufacturer (in mass %) were as follows: $MgCl_2$, 99.98%; Na_2SO_4, 99.99%; K_2SO_4, 99.9%; and $MgSO_4$, 99.95%. Stock solutions were prepared for each salt and analyzed gravimetrically by using silver nitrate for the $MgCl_2$ solution and barium nitrate for the other solutions. All determinations were accurate to ±0.1%. The stock dilutions were diluted either by weighing or volumetrically (±0.1%). As a check on the volumetric dilutions, the concentration after

---

[†] Present address: Division 773.20, National Bureau of Standards, Department of Commerce, Boulder, CO 80303.

0021-9568/83/1728-0056$01.50/0